JOURNAL OF GUIDANCE, CONTROL, AND DYNAMICS
Vol. 32, No. 2, March–April 2009

Extension of the Cucker–Smale Control Law to Space Flight Formations

Laura Perea*
Instituto de Ciencias del Espacio and Institut d'Estudis Espacials de Catalunya (CSIC-IECC), 08034 Barcelona, Spain
Gerard Gómez†
Universitat de Barcelona and Institut d'Estudis Espacials de Catalunya, 08007 Barcelona, Spain
and
Pedro Elosegui‡
Instituto de Ciencias del Espacio and Institut d'Estudis Espacials de Catalunya (CSIC-IECC), 08034 Barcelona, Spain

DOI: 10.2514/1.36269

We designed a spacecraft control law for autonomous formation acquisition and formation keeping. This control law extends the ideas on flight formation for flocks first introduced by Cucker and Smale [Cucker, F., and Smale, S., "Emergent Behavior in Flocks," *IEEE Transactions on Automatic Control*, Vol. 52, 2007, pp. 852–862] by also allowing for particle accelerations, thus incorporating dynamics. When this control law is applied to a multispacecraft system, the resulting formation orbits as a rigid body driven by the natural dynamics of the centroid of the formation. We applied this law to the transfer orbit of a set of spacecraft that, in loose formation, follows a natural trajectory to a libration point orbit, as it is suggested for the Darwin mission. We used two standard metrics to evaluate the performance of this control law: the maximum variation in interspacecraft distance and the integral of the motor thrusts necessary to maintain the formation, or fuel expenditure. For the Darwin case study, the new control law outperforms the zero relative radial acceleration cone control. In particular, we find that the minimum fuel expenditure of the new control law can be 4 orders of magnitude less than the fuel expenditure of zero relative radial acceleration cone control.

I. Introduction

DESIGNING control laws for interacting particle systems is a growing field with applications ranging from spacecraft formation-flying missions [1] to animation simulations in the cartoon industry [2], language modeling [3], biology [4], and many others. In the context of formation-flying missions, many controls have been designed to modify the natural relative dynamics and reach a wide diversity of goals: formation deployment, formation acquisition, formation keeping, reorientation, collision avoidance, etc. Most of the authors probably define controls based on the characteristics of the state transition matrix over the reference trajectory, which gives a natural insight into the movement physics. Although some authors directly use this matrix or the characteristics of its eigenstructure within the controller using ad hoc pole-placement techniques [5–7], others consider optimum control techniques such as the model predictive control [8] and the linear quadratic regulator [9] to minimize a cost function. The potential functions have also been an interesting and elegant tool used by many scientists (e.g., [10,11]) to account for additional mission requirements such as collision avoidance. Less common control strategies can make use of some special manifolds defined by the state transition matrix to define the control [12]. In the interplanetary environment in which the dynamics of the spacecraft are not relevant (i.e., far from planets and libration points), some authors (e.g., [13]) consider free-space dynamics to study basic maneuvers of reorientation, dilatation/contraction, etc. The novelty of the present paper is the extension of a control law that has shown emergent behavior in biology to the spacecraft realm by allowing for the natural relative accelerations.

Of particular interest to this study, Vicsek et al. [14] introduced a simple model of dynamics for a system of particles with biologically motivated interactions. That model assumes that all particles move at the same absolute constant velocity, but their individual headings are driven by the average motion direction of neighboring particles. For this system, they could demonstrate the emergence of self-ordered motion for a range of values of the model parameters. Building on the work of Vicsek et al., Cucker and Smale [3] proposed a model of particle system interactions for which the velocities are fully governed by a distance-decaying law, instead of neighboring interaction law, and they also provided explicit characterization of the sufficient conditions for the system to converge to a common velocity. Shen [15] extended this model to the case of a flock with hierarchical leadership and considered the scenario in which the flock leader may have a freewill acceleration that tends to zero with time. The main goal of the present paper is to extend the Cucker and Smale [3] control law algorithm to a system in which all particles may have a nonzero acceleration. This extension makes the algorithm suitable for autonomous control of a formation of satellites for which the orbits are driven by the dynamics of the environment in space around any reference trajectory.

In this paper, we will focus our interest in formation flying in an interplanetary environment. More explicitly, we are interested in the application of our control law to missions such as Darwin and Terrestrial Planet Finder, which will move close to the collinear libration point L_2 of the sun–(Earth and moon) system. For this purpose, we will use the dynamic model of motion given by the equations of the circular restricted three-body problem (RTBP).

In Sec. II, we summarize the results in [3] that are relevant to this study. In Sec. III, we introduce an extension of the Cucker–Smale

Received 14 February 2008; revision received 27 June 2008; accepted for publication 22 September 2008.

*Research Assistant, Physics and Earth Observation Department, Gran Capità 2-4; perea@ice.csic.es.
†Full Professor, Departament de Matemàtica Aplicada i Anàlisi, Gran Via de les Corts Catalanes 585; gerard@maia.ub.es.
‡Senior Scientist, Physics and Earth Observation Department, Gran Capità 2-4; pelosegui@ice.csic.es.

control law, provide theoretical demonstration for the convergence of the resulting particle system to a formation for which the elements move as a rigid body (i.e., a system for which the particles maintain constant relative distances), and discuss some of the relevant aspects of this control law to highlight its potentials. In Sec. IV, we apply the new algorithm to a spacecraft flight formation, the Darwin mission [16], currently under definition by ESA, and compare results with those obtained with a control law known as zero relative radial acceleration cones (ZRRAC) control developed by Gómez et al. [12].

II. Cucker–Smale Model

The Cucker–Smale model [3] was motivated by the idea that a bird flying in a flock adjusts its velocity toward the average velocity of the flock. To do so, each bird modifies its velocity with a weighted combination of the relative velocities of the rest of birds. The weights are computed as a function of the relative distance, which somehow takes into account the notion that the larger the distance, the lower the accuracy of the relative velocity estimate. Hence, though the neighborhood of each bird is the full space, the influence between birds will tend to zero as the mutual distance increases.

Denoting $x_i(t)$ and $v_i(t)$ as the position and velocity, respectively, of the ith bird of the flock at epoch t, the interaction model is

$$\begin{aligned} x_i(t+1) &= x_i(t) + v_i(t), \\ v_i(t+1) &= v_i(t) + \sum_{j=1}^{k} a_{ij}(v_j(t) - v_i(t)) \end{aligned} \tag{1}$$

where $i = 1, \ldots, k$, and k is the number of birds in the flock. Without loss of generality, it can be assumed that $t \in \mathbb{N}$ and the time span between consecutive velocity updates is $\Delta t = 1$ time unit [3]. The weighting function a_{ij} is defined in [3] as

$$a_{ij} = \frac{K}{(\sigma^2 + \|x_i(t) - x_j(t)\|^2)^{\beta}} \geq 0 \tag{2}$$

where $K > 0$, $\sigma > 0$, and $\beta \geq 0$ are a given set of constants.

Let $x = (x_1, x_2, \ldots, x_k)^T \in \mathbb{R}^{3k}$ and $v = (v_1, v_2, \ldots, v_k)^T \in \mathbb{R}^{3k}$ be the vectors of positions and velocities, respectively, of the birds in the flock, and let $A_x = (a_{ij})$ be the $\mathbb{R}^{k\times k}$ matrix, which we will refer to as the adjacency matrix, with components defined by Eq. (2). Let $D_x \in \mathbb{R}^{k\times k}$ be the diagonal matrix with

$$d_{ii} = \sum_{j=1}^{k} a_{ij}$$

It is easy to check that Eq. (1) can now be written in terms of the Laplacian $L_x = D_x - A_x$ as

$$x(t+1) - x(t) = v(t), \qquad v(t+1) - v(t) = -L_x v(t) \tag{3}$$

where we identified L_x with the $3k \times 3k$ matrix $L_x \otimes I_3$, where I_3 is the identity matrix of dimension 3 and $\otimes$ denotes the Kronecker product. If A is an $m \times n$ matrix and B is a $p \times q$ matrix, then the Kronecker product $A \otimes B$ is the $mp \times nq$ block matrix:

$$A \otimes B = \begin{bmatrix} a_{11}B & \cdots & a_{1n}B \\ \vdots & \ddots & \vdots \\ a_{m1}B & \cdots & a_{mn}B \end{bmatrix}$$

To develop a spacecraft control law, we are specially interested in the continuous version of this model:

$$\dot{x} = v, \qquad \dot{v} = -L_x v \tag{4}$$

where L_x is as before, and we dropped the time variable $t \in \mathbb{R}$ for readability. A remarkable property of the control term $u = -L_x v$ is that it does not affect the common velocity; that is, if all birds have the same velocity $w \in \mathbb{R}^3$, then $v \in \mathbb{R}^{3k}$ is the k replica of the vector w, and $L_x v = 0$. This property will be the key point to define an extension suitable for spacecraft formation flight. For convenience, we will call the continuous system defined by Eq. (4) the Cucker–Smale (C–S) model, which we will use to define a control law for spacecraft formations.

The next theorem is due to Cucker and Smale [3] and characterizes the convergence of the interaction model described in Eq. (4) in terms of the initial conditions and control configuration parameters K, σ, and β.

Theorem by Cucker and Smale [3]. Let $(x(t), v(t)) \in \mathbb{R}^{3k} \oplus \mathbb{R}^{3k}$ be a solution of the system (4) with initial conditions $x(0) = x_0$ and $v(0) = v_0$. Let

$$\Gamma_0 = \frac{1}{2}\sum_{i,j=1}^{k} \|x_i(0) - x_j(0)\|^2$$

and

$$\Lambda_0 = \frac{1}{2}\sum_{i,j=1}^{k} \|v_i(0) - v_j(0)\|^2$$

which are half of the square sum of the relative distances and velocities, respectively. If any of the following conditions regarding the weighting function and the initial relative distances and velocities are satisfied, $\beta < \frac{1}{2}$, $\beta = \frac{1}{2}$ and $\Lambda_0 < (kK)^2/8$, or $\beta > \frac{1}{2}$ and

$$\left[\left(\frac{1}{2\beta}\right)^{\frac{1}{2\beta-1}} - \left(\frac{1}{2\beta}\right)^{\frac{2\beta}{2\beta-1}}\right]\left(\frac{(kK)^2}{8\Lambda_0}\right)^{\frac{1}{2\beta-1}} > 2\Gamma_0 + \sigma^2$$

then when $t \to \infty$, the velocities $v_i(t)$ tend to a common limit $\hat{v} \in \mathbb{R}^3$ and the vectors $x_i - x_j$ tend to a limit vector $\hat{x}_{ij}$, for all $i, j \leq k$:

$$\Lambda(t) \leq \mathcal{O}(e^{-Bt}), \qquad \Gamma(t) \leq \mathcal{O}(e^{-Bt})$$

for certain $B > 0$.

The flock will converge to a common velocity and fly as a formation when the rate of decrease of the weights a_{ij} as the distance decreases is sufficiently slow to allow for the relative velocities to cancel. Thus, if β is less than $\frac{1}{2}$, the relative velocities will decrease fast enough to be cancelled, regardless of the initial relative distances and velocities between elements of the flock. For larger β values, the initial relative positions, relative velocities, and weighting function parameters (K, σ, and β) must satisfy some initial conditions, otherwise, the flock may split into several smaller flocks.

As shown in [15], this result can be easily extended to different definitions of the weighting functions a_{ij} as long as the weights remain bounded:

$$a_{ij} \geq \frac{K}{(\sigma^2 + \|x_i - x_j\|^2)^{\beta}}$$

for certain $K > 0$, $\sigma > 0$, and $\beta \geq 0$.

Remark. Some minor differences can be found in the formulation of theorem as presented here with respect to the formulation in [3]. This is due to some additional properties of the inner product $Q(u, v)$ that are not discussed in [3]. With the notation used in that paper, the inner product $Q(u, v)$ can be written as $u^T Q v$, where Q is the following matrix:

$$Q = \frac{1}{2}\begin{pmatrix} k-1 & -1 & -1 & \cdots \\ -1 & k-1 & -1 & \cdots \\ -1 & -1 & k-1 & \cdots \\ \vdots & \vdots & \vdots & \end{pmatrix} \otimes I_3$$

Using this representation for the inner product, it is straightforward to demonstrate that the parameters ν and $\bar{\nu}$ appearing in the convergence theorem in [3] are equal to $k/2$: that is, $\nu = \bar{\nu} = k/2$.

III. Extension of the Cucker–Smale Model to Flight Formations

In this section, we will demonstrate that based on the C–S model, a control law for a satellite flight formation can be defined. Moreover,

under the same conditions as those of the Theorem by Cucker and Smale [3], it can be guaranteed that the formation will tend to move as a rigid body following the dynamics of its geometric center.

A. Definition of the New Control Law

Consider a set of k satellites that we would like to keep in formation. Let $x_i(t)$ and $v_i(t)$ (for $i = 1, 2, \ldots, k$) be the positions and velocities of each satellite in a given reference frame and define, as before,

$$x = (x_1, x_2, \ldots, x_k)^T \in \mathbb{R}^{3k}, \qquad v = (v_1, v_2, \ldots, v_k)^T \in \mathbb{R}^{3k}$$

We will denote $x_B(t)$ and $v_B(t)$ as the position and velocity of the geometric center, respectively; that is,

$$x_B = \frac{1}{k}\sum_{i=1}^{k} x_i, \qquad v_B = \frac{1}{k}\sum_{i=1}^{k} v_i$$

For any force function $f(x, v)$ and control function $u(x, v)$, we can consider the dynamics of the fleet as

$$\dot{x} = v, \qquad \dot{v} = f(x, v) + u(x, v)$$

If we define the extension of the Cucker–Smale control law as

$$u(x, v) = -L_x v + f(x_B, v_B) - f(x, v) \tag{5}$$

the system reduces to

$$\dot{x} = v, \qquad \dot{v} = -L_x v + f(x_B, v_B) \tag{6}$$

where L_x is the Laplacian of the adjacency matrix A_x. In this definition, x_B and v_B stand for the k replicas, respectively,

$$(x_B, \ldots, x_B)^T \in \mathbb{R}^{3k}, \qquad (v_B, \ldots, v_B)^T \in \mathbb{R}^{3k}$$

We will prove that by using this control law, the formation will tend to move as a rigid body following the dynamics of the centroid. Consider the following decomposition of the position and velocity vectors:

$$x = x_B + \Delta x, \qquad v = v_B + \Delta v$$

Then

$$\frac{\mathrm{d}}{\mathrm{d}t}(x_B + \Delta x) = \dot{x} = v = v_B + \Delta v$$

Because $L_x(v_B, \ldots, v_B)^T = 0$,

$$\frac{\mathrm{d}}{\mathrm{d}t}(v_B + \Delta v) = \dot{v} = -L_x v + f(x_B, v_B) = -L_x \Delta v + f(x_B, v_B)$$

This system is equivalent to the union of the following two independent systems:

$$\begin{cases} \dot{x}_B = v_B \\ \dot{v}_B = f(x_B, v_B) \end{cases} \tag{7}$$

and

$$\begin{cases} \frac{\mathrm{d}}{\mathrm{d}t}(\Delta x) = \Delta v \\ \frac{\mathrm{d}}{\mathrm{d}t}(\Delta v) = -L_x \Delta v \end{cases} \tag{8}$$

By analogy between systems (4) and (8), the Theorem by Cucker and Smale [3] gives sufficient conditions for the system described by the latter to achieve full cancellation of the relative velocities and converge to a flight formation. Unlike Eq. (4), the velocities in Eq. (8) are relative to the velocity v_B of the geometric centroid of the formation. The orbit of the formation centroid, described by Eq. (7), remains effectively decoupled from the performance of the Cucker–Smale control law.

B. Parallel Computation of the New Control Law

A desirable feature of the C–S model is that it does not require intervehicle communications for the computation of the control function u under a certain set of hypotheses on the availability of navigation information. Notice that depending on the navigation system, communications may be required to make navigation information available to individual spacecraft. However, the intervehicle communications necessary for navigation are strongly dependent on the navigation system (sensors and estimator algorithm), and therefore they are outside the scope of this study. The computation of the control maneuvers u necessary to keep the formation entails the computation of two terms: $L_x v$ and $f(x_B, v_B) - f(x, v)$ [see Eq. (5)]. In this section, we discuss when and how each of these two terms can be computed in parallel.

The acceleration necessary to keep satellite i in formation is

$$u_i = -(L_x v)_i + f(x_B, v_B) - f(x_i, v_i)$$

If w is a k replica of v_i, then $L_x w = 0$ and

$$(L_x v)_i = (L_x v - L_x w)_i = \sum_{j=1}^{k} l_{ij}(v_j(t) - v_i(t)) \tag{9}$$

Thus, the computation of the first term in the control function u does not require the knowledge of absolute positions or velocities, but relative distances between satellites i and j for the computation of l_{ij} and relative velocities $v_i - v_j$. This allows full distribution of the computational load of the first term among all satellites as long as each satellite knows its relative distance and velocity with respect to the rest.

Regarding the computation of the acceleration of satellite i relative to the geometric center $f(x_B, v_B) - f(x_i, v_i)$, we will first assume that each satellite knows its acceleration relative to all other satellites. Under this assumption, it is trivial to see that if one of the satellites of the constellation follows the trajectory of the geometric center ($x_b = x_B$ and $v_b = v_B$ for $b \in \{1, 2, \ldots, k\}$), satellite i can autonomously compute the required acceleration u_i. If no satellite is located at the geometric center of the formation, satellite i can still estimate the acceleration with respect to x_B by measuring the relative accelerations with respect to any other satellite in the formation and can interpolate the relative acceleration function to x_B. Of course, the accuracy of the interpolation will depend on the number of satellites k, the geometry of the formation (with respect to satellite i), and the interpolation method. Depending on the selection of the interpolation method, the load associated with the computation of $f(x_B, v_B) - f(x_i, v_i)$ may be much larger than the computational load required to cancel the relative velocities [i.e., Eq. (9)].

Should the relative accelerations between spacecraft not be part of the navigation data that are made available for control purposes, a linear approximation could be used instead: that is,

$$f(x_i, v_i) - f(x_j, v_j) \approx D_x f(x_B, v_B) \cdot (x_i - x_j) + D_v f(x_B, v_B) \cdot (v_i - v_j) \tag{10}$$

where D denotes the derivative operator. This approximation is extremely common in the literature of relative dynamics (e.g., [7]) and reduces the need for information on relative accelerations to the simpler need of relative positions and velocities, which could be derived as a byproduct of standard navigation systems. The performance of this approximation will obviously depend on the nonlinear terms of f and on the relative distance between spacecraft, which can be assessed using a reference trajectory and a nominal intervehicle distance.

C. Some Considerations Regarding Implementation to Space Missions

Unfortunately, two of the assumptions implied by the extension of the C–S model formulated in Sec. III.A [namely, exercising a continuous control and continuous availability of relative data (distance, velocity, and acceleration) from other elements in the

formation] may not be feasible for a real space mission. A practical solution to overcome these difficulties is to discretize the continuous control, which we consider now.

Let t_{i-1} and t_i be the instants of two consecutive maneuvers and

$$\pi_n = \{t_{i-1} = t_{i,0}, t_{i,1}, \ldots, t_{i,n} = t_i\}$$

a partition of the interval $[t_{i-1}–t_i]$, where, for each time epoch $t_{i,j}$, each satellite can measure relative positions, velocities, and accelerations. Let $\Delta t_{i-1,j} = t_{i,j} - t_{i,j-1}$ be the time span between two consecutive estimates of acceleration. We consider the following approximation for an instant maneuver Δu_i at t_i:

$$\Delta u_i = \int_{t_{i-1}}^{t_i} u(t)\mathrm{d}t \approx \sum_{j=1}^{n} u(t_{i,j})\Delta t_{i,j} \tag{11}$$

This approximation will obviously have an impact on the variation of the intervehicle distances. As an example, if $n = 1$, this variation is commensurate with the error of a first-order ordinary differential equation integrator. The error could then be regulated to a certain extent by a step-size control, as in any integrator routine with step-size control. If $\tilde{x}(t_i)$ is the solution of system (6) and $\hat{x}$ is the result of using Eq. (11) with boundary conditions at t_{i-1} equal to x_{i-1} and v_{i-1}, the difference between the continuous implementation of the control law and its discretized approximation $\tilde{x}(t_i) - \hat{x}(t_i)$ could be used as an indicator of the goodness of the value $\Delta t_m = t_i - t_{i-1}$.

However, an optimal Δt_m depends on the state vector of the vehicles and on the control configuration parameters K, σ, and β. During the evaluation of this control, we found that the optimal Δt_m tends to zero for large configuration values (even if the convergence is guaranteed by the Theorem by Cucker and Smale [3]) and large Δv values at $t = 0$. As introduced earlier, a step-size control could be implemented to use an appropriate Δt_m value, but a realistic onboard implementation will require fixing a minimum value, which can make the approximation in Eq. (11) unsuitable. The larger the Δt_m value compared with the optimum, the worse the performances of the algorithm. We will consider that this approximation has completely disrupted the performances of the algorithm when the final separation among spacecraft is larger than when no control is applied. An example of this behavior can be found in the simulations presented in Sec. IV.C, in which the performances of the algorithm are disrupted because of the discrete approximation in the computation of Δu_i. For this reason, we recommend validating the suitability of large K, σ, and β values for each specific mission with simulations, even if the convergence is guaranteed by the Theorem by Cucker and Smale [3].

Space mission thrusters impose some additional limitations, such as maximum and minimum Δu thresholds, that also warrant some consideration. When the magnitude of the required Δu_i is lower than allowed by mission specifications, the maneuver can be postponed and the algorithm will continue accumulating unperformed maneuvers until the magnitude of the Δu_j $(j > i)$ exceeds the minimum threshold and can be executed. On the other hand, if the Δu_i is larger than is feasible, a maximum maneuver can be performed and the remaining amount of Δu_i will be accumulated for the subsequent maneuver.

The C–S control has been designed as a stabilization law (i.e., to cancel intervehicle velocities and accelerations), but variations of the intervehicle distances may exist due to the convergence process and the approximations described in this section. For a real mission, these variations might violate specific requirements such as maximum/minimum intervehicle separations. To avoid this, the C–S control law could be combined with other appropriate strategies (e.g., collision avoidance) to meet those mission specifications.

IV. Application of the C–S Model to the Transfer Orbit of Darwin

A. Darwin Space Mission

To evaluate the Cucker–Smale control law under a realistic scenario, we performed numerical simulations for one of the mission phases of Darwin, an ESA space mission aimed at scanning the nearby universe for signs of life in Earth-like planets. Darwin will consist of several spacecraft, one of them serving as the communications hub and the rest operating as telescopes. The fleet should reach a halo orbit around the libration point L2 of the sun–Earth system after its launch, which is scheduled for 2015. The mission planning for the transfer from Earth to the halo orbit is still under discussion, with several possibilities under consideration. One favorable option would deploy a fleet of three satellites at the beginning of the transfer. The fleet would then follow an orbit of the stable manifold of the target halo orbit. During the transfer orbit, spacecraft are expected to keep a loose formation (i.e., the relative position and velocity requirements are rather relaxed).

We thus considered a fleet of three spacecraft flying in loose formation along the transfer orbit. To specify the orbits of the fleet, we used two sets of parameters: 1) those that define a reference orbit that is to be followed by one of the spacecraft and 2) the relative distances between the satellite at the reference orbit and the two remaining spacecraft. For convenience, we will refer to the former as the reference satellite and to the latter as outer satellites. As the reference orbit, we selected the transfer trajectory from the Earth to a halo orbit of moderate amplitude ($\sim$150, 000 km) around the equilibrium point L_2 of the sun–(Earth and moon) system. The transfer trajectory is taken in the branch of the stable manifold of the halo orbit that approaches the Earth. Figure 1 shows the transfer orbit as a function of time in the usual synodical reference system and units (see [17]). For the definition of this reference system, we assumed the large primary on the positive X axis and considered the mass parameter $\mu = 0.3040357143 \times 10^{-5}$. The initial state vector is included in Table 1. The transfer orbit, which spans 230 days, was integrated using the RTBP equations with an adaptive Runge–Kutta integrator of orders 4 and 5. The local error bounds for the Runge–Kutta integrator are 0.1% relative to the state vector and 10^{-6} in absolute magnitude.

B. Description of the Experimental Configuration

We performed an extensive set of numerical simulations to evaluate the performance of the new C–S control law defined in Eq. (5) for the study case of the transfer trajectory of the Darwin mission. We considered simulations that explored the impact on performance of a large set of key configuration parameters of both the model and the mission scenario. Parameters K, β, and σ are specific to the C–S model [see Eq. (2)]. On the other hand, parameters d_i, α, β, Δv_0, T_t, N, T_m, NavSet, σ_R, $u_{\min}$, and $u_{\max}$ are specific to the final scenario for the Darwin mission and are defined as follows:

1) The initial distance between the reference satellite and the outer satellites is d_i $(i = 1, 2)$, and it is realistic to assume that for this mission option, $d_1 = d_2$.

2) The initial orientation of the fleet is defined by α and θ. The physical meaning of these parameters will be introduced subsequently, when the control based on ZRRAC is introduced (see Sec. IV.D).

3) The initial relative speed between the reference satellite and the outer satellites is $\|\Delta v_0\|$.

4) The time interval between two consecutive control maneuvers is T_t. A new control maneuver can be started once every T_t time units. Each control maneuver, in turn, consists of N correction maneuvers.

5) The number of correction maneuvers associated with one control maneuver is N. In our simulations, all the correction maneuvers are executed at equal time intervals and are completed in T_m time (discussed subsequently), though a modification of this would be straightforward, but was not deemed to be necessary.

6) The time duration necessary for the completion of all N correction maneuvers associated with one control maneuver is T_m. By definition, $T_m \leq T_t$.

7) NavSet flags the availability (or lack thereof) of relative acceleration data in the navigation data set. In these simulations, we also considered several levels of random noise in the navigation data set. When only relative positions and velocities are available to the controller, an additional parameter σ_R is then to be specified, which indicates the noise level in the navigation data. Thus, we consider the impact of the approximation

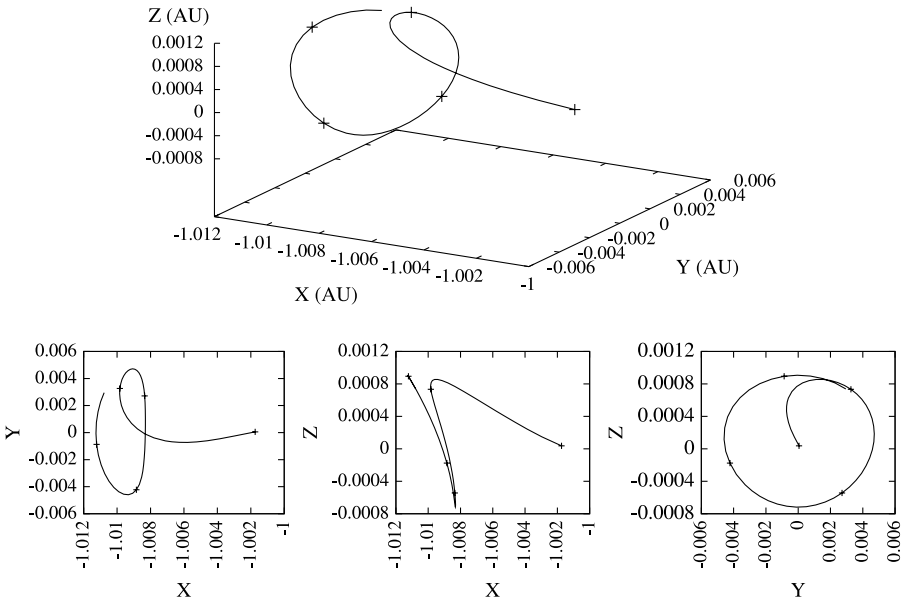

Fig. 1 Three- (top) and two-dimensional (bottom) representation of the reference orbit of the transfer trajectory of the Darwin fleet to an L2 halo orbit. All axes are in astronomical units. Time interval of 50 days are marked by crosses. The orbit direction goes from right to left in the all representations except in the *Y–Z* representation, in which it goes from the center of the graph to the edge. Note the scale change in the *Z* axis.

$$f(x_i, v_i) - f(x_j, v_j) \approx Df(x_B) \cdot (x_i - x_j) + w$$

where

$$w \sim N\left(0, \begin{pmatrix} \sigma_R \cdot I_3 & 0_3 \\ 0_3 & 0.01 \cdot \sigma_R \cdot I_3 \end{pmatrix}\right)$$

that is, the noise of the relative positions is a zero-mean Gaussian variable with standard deviation σ_R, and the noise in the relative velocities is assumed to be 1% of σ_R. A $\sigma_R = 0$ indicates noiseless simulations.

8) The limitations imposed by the spacecraft thrusting system are $u_{\min}$ and $u_{\max}$ (i.e., the minimum and maximum magnitude tolerated for thruster acceleration, respectively).

Each simulation covered the 230 days necessary to travel the length of the transfer orbit (Fig. 1). We performed a set of simulations for each one of the parameters defined earlier. In each set of simulations, all the parameters except one were kept fixed. This test parameter was changed to within a predetermined range from simulation to simulation, during which its value was kept fixed. We then used two standard metrics to evaluate the performance of the application of the new C–S control law to the Darwin mission, $\max(\Delta d)$ and total Δv, defined as follows:

1) The maximum variation of the intersatellite distances is $\max(\Delta d)$; that is, if $d_i(t)$ is the distance between the reference satellite and one outer satellite at time t, the maximum variation at all times is $\max t|d_i(t) - d_i(0)|$ for $i = 1, 2$.

2) The integral of the accelerations required to keep the flight formation is total $\Delta v = \int u\mathrm{d}t$; that is,

$$\int |u(x, v)|\mathrm{d}t = \sum_i |\Delta u_i|$$

Table 1 Initial state vector of the transfer orbit in RTBP adimensional coordinates

State vector	AU
x_0	−1.00174076
y_0	0.00005287
z_0	0.00003747
$\dot{x}_0$	−0.05015739
$\dot{y}_0$	−0.01136307
$\dot{z}_0$	0.00399552

where Δu_i are the instantaneous correction maneuvers. This metric is sometimes referred to as both the cost and the fuel expenditure in the literature. We will use these two terms interchangeably.

To maintain consistency throughout the simulations and to facilitate the interpretation of the results, we defined a baseline scenario and modified the value of only one parameter from one test to the next whenever possible. There are cases in which it was necessary to change more than one parameter at a time: for example, in the case of parameters K, σ, and β. Thus, $\|\Delta v_0\|$ was set to a fixed, and significantly large, value in the tests involving the three parameters to test the performances of the term $L_x v$ under a nonfavorable scenario. But we assumed that $\|\Delta v_0\| = 0$ for the rest of tests to decouple the effect of Δv_0 and the parameter under experimentation and to consequently ease the interpretation of the results of each test separately. To allow direct comparison of the C–S results with the results presented in [18] using the ZRRAC strategy, we introduced other minor differences with respect to the baseline scenario to the tracking time T_t, number of maneuvers N, and maneuver time T_m.

C. Example of a Representative Set of Numerical Simulations

In this section, we present a set of numerical simulations for the case in which the value of the model parameter β changes but the rest of parameters remain unchanged. Each simulation in this set will use a different value of β, ranging from 0 to 2. We selected these simulations to exemplify performance because the emergence of cooperative behavior in the C–S model critically depends on the value of this particular parameter [3]. For conciseness, we will focus on this simulation set herein and an additional simulation that involves a comparison to an independent control model in the next section, and we will defer the presentation of the simulations for all the other parameters tested to Appendix A. For completeness, we will summarize the main results from all simulations, including those in Appendix A, in the last section.

Table 2 lists the choice of parameter values used in this set of simulations, the results of which are shown in Fig. 2. This figure shows, as a function of β, the variation of the two metrics used to evaluate performance: $\max(\Delta d)$ and total Δv. The overall character of both metrics is similar, initially decreasing their value from $\beta = 0$ to a minimum at $\beta = 0.4$, then gradually increasing throughout $\beta = 1$ and plateauing thereafter.

At first glance, the decreasing character of both metrics for β values smaller than 0.4 may seem somewhat surprising. However,

Table 2 Values of the configuration parameters (brackets denote an interval of parameter values)

K	β	σ	d_i, m	α, deg	θ, deg	$(\|\Delta v_0\|/v_B)\cdot 100$, %	T_t, h	N	T_m, h	NavSet[a]	$u_{\min}$, m/s^2	$u_{\max}$, m/s^2
Simulations with parameter β												
10^{-4}	[0–2]	6.7×10^{-10}	10^3	0	35.23	10^{-3}	2	10	2	$\surd$	0	∞
Simulations with parameter T_m												
10^{-4}	0.3	6.7×10^{-10}	10^3	0	35.23	0	6	10	[1–5]	$\surd$	0	∞

[a]The symbol $\surd$ indicates that relative positions, velocities, and accelerations are available.

although the Theorem by Cucker and Smale [3] guarantees convergence of the spacecraft velocities exponentially on time, the coefficient B of the exponential term in the Theorem by Cucker and Smale [3] may also be small for β values close to 0, thus slowing down the convergence. Accordingly, inspection of Eq. (2) reveals that for $\sigma^2 \ll 1$ and $||x_i - x_j||^2 \ll 1$, the smaller the β value, the smaller the weighting terms a_{ij}, which thus translates into a slower convergence. Notice that the previous condition $||x_i - x_j||^2 \ll 1$ holds during the entire transfer orbit when using astronomical units. This means that the usage of the control law (5) with these configuration values effectively cancels the relative accelerations $f(x_B, v_B) - f(x, v)$ but slightly affects the initial relative velocity, which results in a constant increase of the relative positions $x - x_B$ ($\sim 3\times10^5$ m over 230 days). Regarding the total Δv associated with this range of configuration values, it seems reasonable that the more the intervehicle separation increases as a function of time, the larger the maneuvers would have to be. Therefore, it seems logical that the β value that minimizes the intervehicle distance variation coincides, at least in first approximation, with the β value that minimizes the total Δv.

For β values larger than 0.5, the third condition in the Theorem by Cucker and Smale [3] still holds, however, the weights a_{ij} decrease too rapidly as a function of the intervehicle distances $||x_i - x_j||$, requiring Δt_m (T_m/N in these simulations) to tend to 0 as β increases. Therefore, the discrete computation of instantaneous control accelerations becomes inappropriate for large β values and disrupts the performances of the control strategy. Excessive discrete maneuvers are constantly applied, leading to an intervehicle separation larger than before each maneuver. For $\beta \geq 0.8$, the maximum separation is even larger than 10^8 m, which is the maximum separation among satellites after the 230 days of free flight over the transfer orbit. Accordingly, the associated total Δv is exaggeratedly large:

$$\sim 10^{15}\ \text{m}/230\ \text{days} = 5.03\times10^6\ \text{m/s}$$

D. Performance Comparison of Two Independent Control Law Models

For comparison purposes, we also present a set of simulations for the Darwin mission performed with two independent control models: C–S and the model by Gómez et al. [12]. The authors developed a control law model based on ZRRAC and applied it to the Darwin flight formation problem. They showed that there is a cone of zero relative radial acceleration for each point along the Darwin transfer trajectory. This control law is thus based on positioning the reference satellite on the trajectory of the Darwin transfer orbit, as was the case for the implementation of the preceding C–S model and the two outer spacecraft on these cones, in which the relative radial acceleration vanishes. Because these cones are not invariant by the natural dynamics in space, a control is necessary to bring the satellites back to the cones. Any point on the cone can be defined by the angle α of the generatrix in which it lies and a distance d to the vertex of the cone, which can be positive or negative. The merit of the ZRRAC strategy is that as time evolves, the three spacecraft remain aligned on the generatrix of angle α and their mutual distances remain constant. The additional parameter θ previously introduced in the definition of the configurations is the initial angle between the relative position of the outer spacecraft and the axis of the ZRRAC. If the spacecraft is initially on a ZRRAC, $\theta = 35.23$ deg.

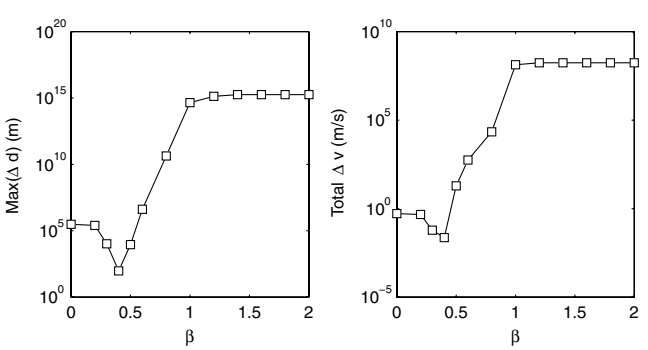

Fig. 2 Variation versus model control parameter β of the maximum variation of the intersatellite distance (left) and the total Δv (right).

To compare the performances between both controls, we selected the simulations corresponding to the parameter T_m, the time duration for the execution of a control maneuver, and for conciseness, we defer the rest of the simulations to Appendix A. Although we selected T_m, any common parameter could have been chosen to illustrate the comparison of models.

The experimental configuration of these simulations coincides with the configurations in [18] to ease the comparison of results and is similar to those in Table 2, with a few necessary exceptions. Parameter T_m, the focus of this set, will vary between 1 and 5 h. Parameter T_t is increased to 6 h to accommodate the experimental requirement that $T_m \leq T_t$. The β parameter is set to 0.3, which was the original value for the baseline configuration, and it was a reasonable value, close to the optimum according to the previous simulation. Notice that the optimum set of configuration parameters may not be the set of individual optimum values, and thus finding the optimum set was out of the scope of this study. The goal of these tests was not to find an optimal configuration parameter, but to address the dependence of the performances on these parameters. Because the goal of the ZRRAC strategy is to keep a formation, more than acquiring a formation, $\|\Delta v_0\|$ was consequently set to 0, which is the main configuration difference with respect to the previous test. Notice that the variation of the $\|\Delta v_0\|$ setup does not allow direct comparison of the results presented in previous section and those obtained for this test. The dependence of the algorithm performances on this additional parameter will be discussed in detail in Sec. V. For completeness, Table 2 also lists the choice of parameter values used in this set of simulations.

Figure 3 shows that the maximum variation of intersatellite distance $\max\{\Delta d\}$ in the C–S model is smaller than in the ZRRAC model, except for T_m smaller than $2h$. Notice that in such a case, $\max\{\Delta t_m\} = T_t - T_m \geq 4h$. As could be expected from the approximation in Eq. (11), both the intervehicle variation and the total Δv decrease as $\max\{\Delta t_m\} = T_t - T_m = 6 - T_m$ decreases and the approximation becomes more accurate. The special benefit of the C–S control compared with the ZRRAC is total Δv, which is at least 3 orders of magnitude smaller when using the C–S control. Though the ZRRAC control law minimizes relative radial acceleration, these cones are not invariant by the dynamics, and the total Δv for the ZRRAC strategy mostly arise from repositioning the satellites on these cones. On the other hand, the cost of the C–S control is mainly due to the cancellation of the relative accelerations

$$\int u\mathrm{d}t \approx \int (f(x_B, v_B) - f(x, v))\mathrm{d}t$$

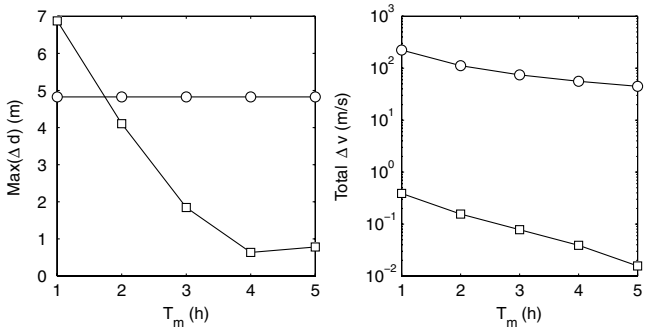

Fig. 3 Same as Fig. 2, except for the time duration for the execution of a control maneuver T_m for the C–S model (squares) and the ZRRAC model (circles).

because $\Delta v_0 = 0$, which seems to be several orders of magnitude lower than the fuel expenditure required to keep the spacecraft on these noninvariant cones.

V. Results

The main results of the two sets of simulations presented earlier, as well as the simulations in Appendix A, can be summarized as follows:

1) The combination of small K and β values with large σ values leads to small, almost constant, weights a_{ij} as a function of the intervehicle distance, which results in a Cucker–Smale model that is extremely slow to converge. This means that the usage of the control law (5) with these configuration values effectively cancels the relative accelerations $f(x_B, v_B) - f(x, v)$ but slightly affects the initial relative velocity, which results in a constant increase of the relative positions $x - x_B$ ($\sim 3 \times 10^5$ m after 230 days).

Instead, for large K and β values and small σ values (and as long as the convergence is guaranteed), the optimal Δt_m may tend to zero. The alternative of using a fixed Δt_m larger than zero may disrupt the performances of the algorithm, as can be observed in Figs. 2 and A1. The application of a discrete maneuver for too long may result in excessive thrusting that would lead to an intervehicle separation larger than the initial separation. For the largest values of K and β, the maximum separation after 230 days is even larger than 10^8 m, which is the maximum separation among satellites after the 230 days of free flight. According to this, the total Δv associated with the control is exaggeratedly large.

When testing the σ parameter, the large baseline K value does not let the algorithm reach relative velocities close to 0, which in turn minimizes the effect of a small σ value in the denominator of the weights in Eq. (2) (see Fig. A2). However, for smaller K and σ values, some instabilities could be expected when the intervehicle distances are small compared with the σ value. This result highlights the dependence of the optimum value of a parameter on the value of the other parameters.

An interesting result is that the configuration values that result in the lowest intervehicle variation are also those that require less fuel expenditure, because the terms Δx, Δv, and $f(x_B, v_B) - f(x, v)$ are lower during most of the transfer orbit. For the case of the Darwin transfer orbit, the individual optimum values for β, K, and σ have been found to be around 0.4, 0.01, and less than $\sim 10^{-8}$, respectively.

2) The dependence of the two metrics on the initial intervehicle distance is linear (see Fig. A3), consistent with simulation results obtained by other authors for the relative dynamics between two spacecraft in space [12].

3) As could be expected from the definition of the ZRRAC, changes in the initial relative directions within the corresponding ZRRAC, or α parameter, have a small and periodic effect on the performance of both controls. The maximum variation of the intervehicle distances ranges between 1–3 m, and the total Δv is ~ 0.016 m/s for the C–S control (see Fig. A4).

On the other hand, changes in the angle with respect to the axis of the ZRRAC, or θ parameter, have a slightly larger impact on the two metrics, because this angle will range from the maximum relative radial acceleration direction to the minimum. In these simulations, the maximum variation of the intervehicle distances ranges from 2 to 22 m, and the total Δv ranges from ~ 0.011 and ~ 0.022 m/s (see Fig. A5).

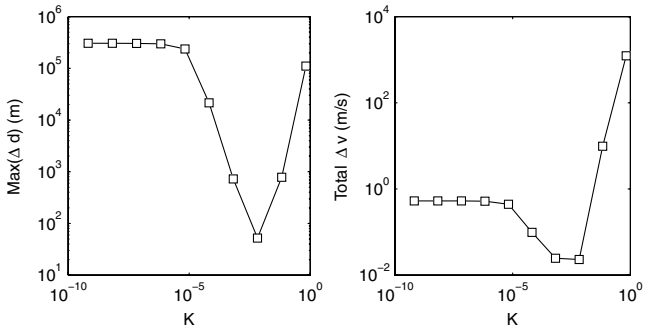

Fig. A1 Same as in Fig. 2, except for parameter K.

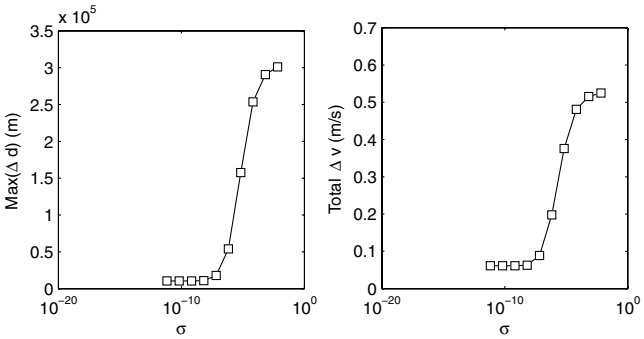

Fig. A2 Same as in Fig. 2, except for parameter σ.

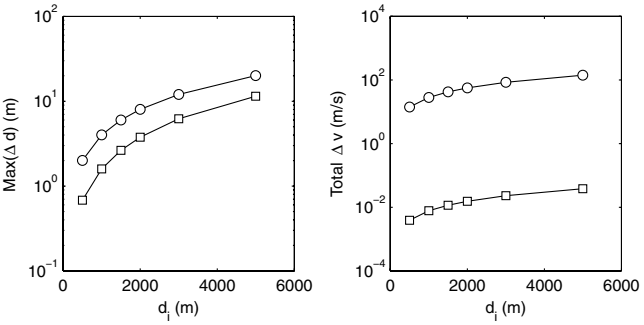

Fig. A3 Same as in Fig. 3, except for parameter d_i. The logarithmic scale has been used for the vertical axis to allow comparison between performances of both control laws. When plotted in linear scale, a linear dependence with respect to d_i can be clearly observed.

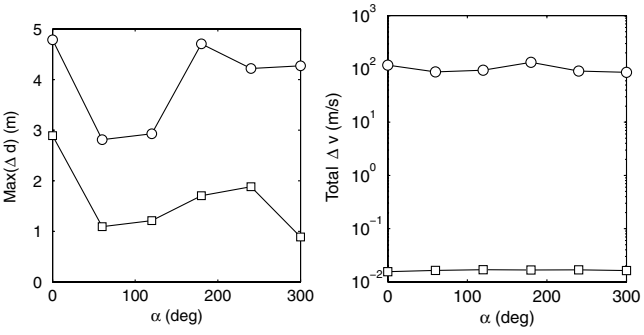

Fig. A4 Same as in Fig. 3, except for parameter α.

4) Regarding the impact of the initial relative velocities under the baseline configuration, the C–S algorithm is fast enough to cancel the relative velocities before the relative distances increase significantly, as long as $\|\Delta v_0\| < 10^{-6}\%$ of the absolute velocity of the centroid, $v_B(0)$. For these cases, the cost of the C–S control is mainly due to the cancellation of the relative accelerations: that is,

$$\int u\mathrm{d}t \approx \int [f(x_B, v_B) - f(x, v)]\mathrm{d}t = \mathcal{O}(10^{-2}) \text{ m/s}$$

For initial relative velocities between 10^{-6} and $10^{-4}\%$, the relative distances have already increased before the algorithm converges; however, the total Δv remains almost constant. For larger initial relative velocities, the relative distance increases so fast as a function of time that it becomes more expensive in terms of Δv to cancel the relative dynamics (see Fig. A6).

5) We used parameters T_t, N, and T_m to define an experimental configuration because they are easy to understand and are common in the literature. However, the maximum time between consecutive maneuvers, $\Delta t_m = \max(T_m/N, T_t - T_m)$, is a better parameter for the evaluation of the performance of the Cucker–Smale model. We found that the maximum separation and the total Δv of the C–S model critically depends on Δt_m. When the frequency of maneuvers is higher, Eq. (11) is more accurate and the maximum variation of intervehicle distances and total Δv are lower. Using $\Delta t_m \leq 1h$ seems to have a negligible impact on the total Δv (see Figs. 3, A7, and A8). Thus, a high frequency of maneuvers may reduce the maximum variation of the intervehicle distance without increasing the cost of the maneuvers, or total Δv.

Relative navigation information (i.e., relative positions and relative velocities) needs to be available to each spacecraft, at least at the same frequency as the maneuver's frequency. Fortunately, the

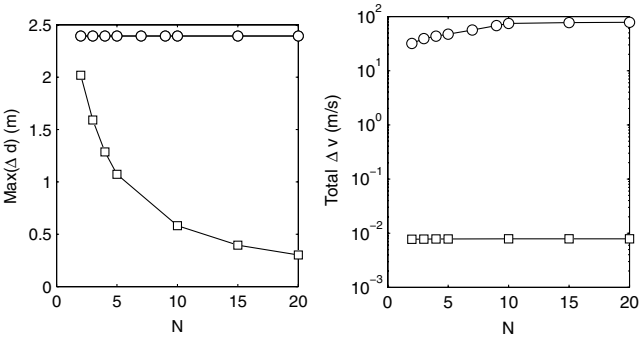

Fig. A8 Same as in Fig. 3, except for parameter N.

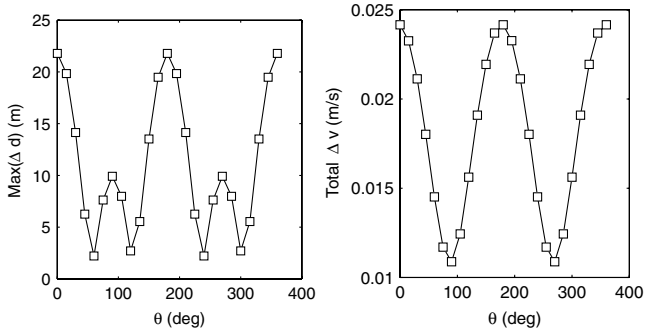

Fig. A5 Same as in Fig. 2, except for parameter θ.

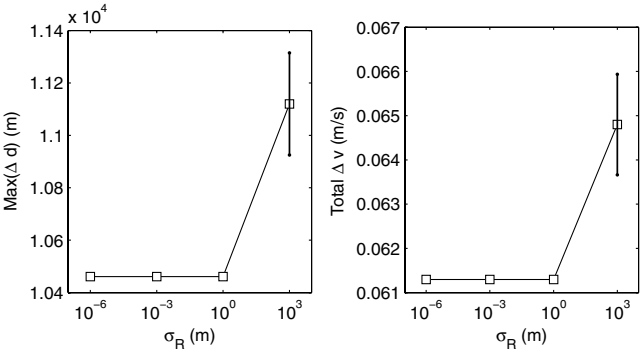

Fig. A9 Same as in Fig. 2, except for parameter σ_R.

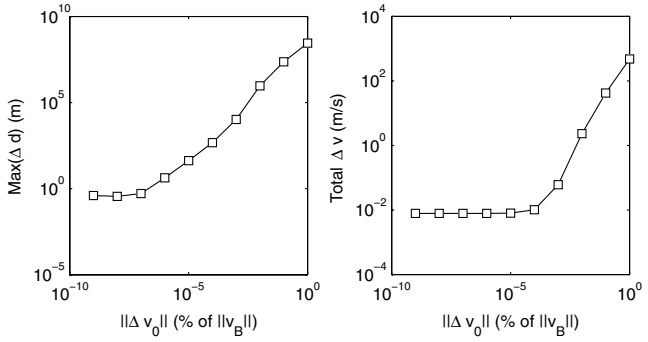

Fig. A6 Same as in Fig. 2, except for parameter $\|\Delta v_0\|$.

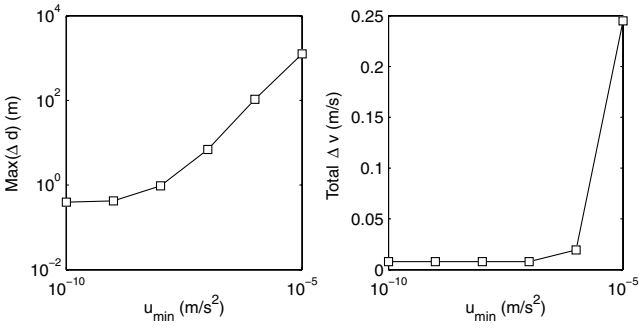

Fig. A10 Same as in Fig. 2, except for parameter $u_{\min}$.

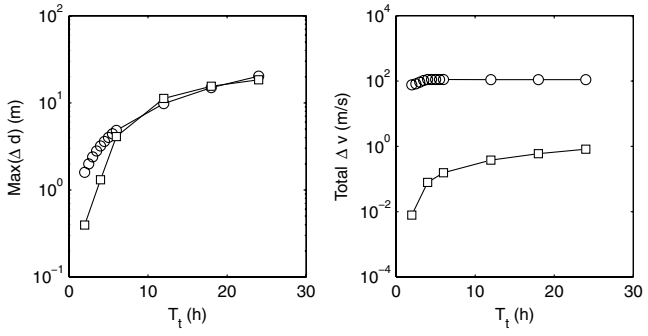

Fig. A7 Same as in Fig. 3, except for parameter T_t.

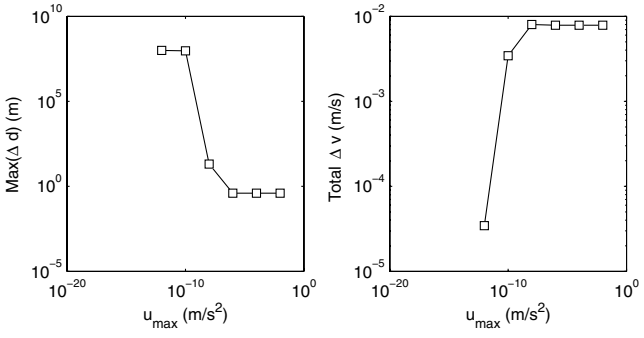

Fig. A11 Same as in Fig. 2, except for parameter $u_{\max}$.

Table A1 Values of the configuration parameters

K	β	σ	d_i, m	α, deg	θ, deg	$(\|\Delta v_0\|/v_B)\cdot 100$, %	T_t, h	N	T_m, h	NavSet[a]	$u_{\min}$, m/s^2	$u_{\max}$, m/s^2
Cucker–Smale configuration parameter K												
$6.7\times[10^{-10}$–$0.1]$	0.3	6.7×10^{-10}	10^3	0	35.23	10^{-3}	2	10	2	√	0	∞
Cucker–Smale configuration parameter σ												
10^{-4}	0.3	$6.7\times[10^{-12}$–$10^{-3}]$	10^3	0	35.23	10^{-3}	2	10	2	√	0	∞
Spacecraft initial separation d_i												
10^{-4}	0.3	6.7×10^{-10}	[500–5000]	0	35.23	0	2	2	2	√	0	∞
Angle α												
10^{-4}	0.3	6.7×10^{-10}	10^3	[0–300]	35.23	0	2	2	2	√	0	∞
Angle θ												
10^{-4}	0.3	6.7×10^{-10}	10^3	0	[0–360]	0	2	10	2	√	0	∞
Relative speed $\|\Delta v_0\|$												
10^{-4}	0.3	6.7×10^{-10}	10^3	0	35.23	$[1$–$10^{-9}]$	2	10	2	√	0	∞
Tracking time interval T_t												
10^{-4}	0.3	6.7×10^{-10}	10^3	0	35.23	0	[2–24]	10	2	√	0	∞
Number of maneuvers N												
10^{-4}	0.3	6.7×10^{-10}	10^3	0	35.23	0	3	[2–20]	3	√	0	∞
Simulations including navigation noise σ_R ($[10^{-6}$–$10^3]$ m)												
10^{-4}	0.3	6.7×10^{-10}	10^3	0	35.23	10^{-3}	2	10	2	×	0	∞
Lower thruster limitation $u_{\min}$												
10^{-4}	0.3	6.7×10^{-10}	10^3	0	35.23	0	2	10	2	√	[10^{-10}–10^{-5}]	∞
Higher thruster limitation $u_{\max}$												
10^{-4}	0.3	6.7×10^{-10}	10^3	0	35.23	0	2	10	2	√	0	$[10^{-12}$–$10^{-2}]$

[a]The symbol √ indicates that relative positions, velocities, and accelerations are available. The symbol × indicates that only relative positions and velocities are available to the controller. In this case, σ_R will range from 10^{-6} to 10^3.

availability of this information is deemed to be a reasonable assumption for frequencies larger than minutes.

6) Approximating relative accelerations by the linearized dynamics [Eq. (10)] has a negligible effect on the control performances. Also, introducing Gaussian noise to represent random errors in the navigation data set (estimates of relative positions and velocities) does not seem to have a significant impact as long as σ_R is not larger than 1 m (see Fig. A9). As an example, $\sigma_R = 1$ m results in a standard deviation for both metrics lower than $\sim 10^{-3}\%$. This result indicates that the combined error due to the linearization and the observer noise has a much lower impact than the error due to the discrete control update.

7) Experimentation with different values for the thrusters limitations indicate the range of accelerations required during most of the transfer orbit and the accelerations required by the C–S algorithm to provide reasonable performances. According to current simulations, thrusters should be able to cope with accelerations ranging from 10^{-8} to 10^{-6} m/s^2 continuously, which means that micronewton thrusters or, equivalently, instantaneous impulses from $\sim 10^{-6}$ to $\sim 10^{-4}$ m/s every 12 min may be necessary (see Figs. A10 and A11).

8) The C–S model provides slightly better performances than the ZRRAC in terms of maximum intervehicle separation for most of the configurations tested. The special benefit of the C–S is that it always requires several orders of magnitude less fuel expenditure than the ZRRAC. As an example, the total Δv can be reduced to 0.01% of the cost of the ZRRAC if the maximum time between consecutive maneuvers is less than 1 h; that is,

$$\max\{\Delta t_m\} = \max\{T_m/N, T_t - T_m\} < 1h$$

Although the ZRRAC control law minimizes relative radial acceleration, these cones are not invariant by the dynamics, and the total Δv for the ZRRAC strategy mostly arise from repositioning the satellites on these cones. On the other hand, the cost of the C–S control is mainly due to the cancellation of the relative accelerations

$$\int u \mathrm{d}t \approx \int (f(x_B, v_B) - f(x, v))\mathrm{d}t$$

when $\Delta v_0 = 0$, which seems to be several orders of magnitude smaller than the fuel expenditure required to keep spacecraft on these noninvariant cones (see Figs. 3, A3, A4, A7, and A8).

VI. Conclusions

We extended the Cucker–Smale model for particle system interaction to control a formation of satellites. Based on the C–S algorithm, we defined a control model that cancels the relative dynamics (between satellites) and decreases the initial relative velocities to zero. We proved the validity of this control model analytically based on the results of Cucker–Smale convergence analysis, and we provided sufficient conditions for the formation to move as a rigid body.

We discussed the conditions for a parallel implementation of this strategy between all satellites, thus minimizing the communications requirements of a real mission. If each satellite can estimate its relative distance, velocity, and acceleration to any other satellite in the space formation, the control can be completely parallelized. These are not uncommon conditions for a formation intended to navigate autonomously.

To finalize the general discussion of the C–S model for flight formations, we made some additional considerations for the implementation of the C–S model in a realistic environment in which some limitations arise. In this scope, we discussed the observation's availability and the limitations due to thrusters constraints (the unsuitability of using thrusters continuously and the maximum and minimum limitations of the thrusting system). Thus, we proposed some approximations to the C–S model and assessed the associated errors. Experience has revealed that configuration parameters β, K, and σ have a significant impact on the performances of this control law. The optimum values may depend on the dynamics (f function) and other control configuration parameters such as the maximum time between consecutive correction maneuvers. These parameters can be tuned based on mission requirements and realistic simulations.

As an application of this control law, we simulated the orbit of the transfer phase of the Darwin mission and applied the new C–S model to control the formation. In this phase, three satellites are supposed to take a transfer orbit to leave an Earth orbit and reach a halo orbit around the libration point L2. Several initial conditions have been tested to address the dependence of this control on the main configuration parameters under a realistic scenario. Some of these results have been also compared with the ZRRAC control model [12].

The most remarkable conclusions of the tests are summarized as follows:

1) The performance of the new control law is particularly sensitive to the values of the configuration parameters K, β, and σ and two mission-specific parameters $\|\Delta v_0\|$ and $\Delta t_m = \max\{T_t - T_m, T_m/N\}$. Thus, a global optimum will strongly depend on the specific mission configuration for which this control law might be used.

2) The configuration values K, β, and σ that minimize the intervehicle distance variation coincide, at first approximation, with the values that minimize the total Δv.

3) The control strategy is robust against Gaussian errors from the relative navigation data set (relative positions and velocities).

4) In general, the C–S strategy performs better than ZRRAC in terms of maximum spacecraft separation. The advantage of the C–S model over the ZRRAC model is that it always requires several orders of magnitude less fuel expenditure.

Appendix A: Simulation Results of a Complete Set of Parameters

We present a comparative analysis of the performances of the Cucker–Smale and the ZRRAC control laws for the Darwin mission under different configurations. Each set of simulations contains an assessment of the control law performances with respect to each of the parameters described in Sec. IV.B. The simulations presented include the Cucker–Smale configuration parameter K and σ, the spacecraft initial separation d_i, the angle α, the angle θ, the relative speed $\|\Delta v_0\|$, the tracking time interval T_t, the number of maneuvers N, the navigation noise level σ_R, the lower thruster limitation $u_{\min}$, and the higher thruster limitation $u_{\max}$.

Table A1 summarizes the scenario of each specific simulation under consideration. Figs. A1–A11 show the maximum variation of the intervehicle distance and the total cost required to apply the Cucker–Smale algorithm and the ZRRAC control, the latter when applicable, for all possible scenarios and parameter values. Results are presented in Sec. V.

The set of simulations involving the navigation noise σ_R depends on the random variable w, which simulates random errors in the navigation system. We ran 100 simulations for each configuration and computed the mean and standard deviation of the results, which are shown in Fig. A9. For each noise level, the square symbol represents the mean value and the error bar represents the one standard deviation. For $\sigma_R = 1$ m or smaller, the error bars are smaller than the symbol and thus are not visible.

Acknowledgments

This work was supported by Spanish Ministry of Education and Science (MEC) fellowship BES-2005-8607 (LP) and MEC grants ESP2004-00218 and ESP2007–62680. Suggestions from three anonymous reviewers and the Associate Editor Hanspeter Schaub significantly improved this manuscript.

References

[1] Marcote, M., "Vuelo en Formación de Constelaciones de Satélites," M.S. Thesis, Facultat de Matemàtiques, Univ. de Barcelona, Barcelona, Sept. 2002.

[2] Reynolds, C. W., "Flocks, Herds and Schools: A Distributed

Behavioral Model," *Proceedings of the Annual Conference on Computer Graphics and Interactive Techniques (SIGGRAPH'87)*, Vol. 21, ACM Press, New York, 1987, pp. 25–34.

[3] Cucker, F., and Smale, S., "Emergent Behavior in Flocks," *IEEE Transactions on Automatic Control*, Vol. 52, No. 5, May 2007, pp. 852–862. doi:10.1109/TAC.2007.895842

[4] Couzin, I. D., Krause, J., Franks, N. R., and Levin, S. A., "Effective Leadership and Decision Making in Animal Groups on the Move," *Nature*, Vol. 433, No. 7025, Feb. 2005, pp. 513–516. doi:10.1038/nature03236

[5] Scheeres, D. J., Hsiao, F. Y., and Vinh, N. X., "Stabilizing Motion Relative to an Unstable Orbit: Applications to Spacecraft Formation Flight," *Journal of Guidance, Control, and Dynamics*, Vol. 26, No. 1, 2003, pp. 62–73. doi:10.2514/2.5015

[6] Hsiao, F. Y., and Scheeres, D. J., "Design of Spacecraft Formation Orbits Relative to a Stabilized Trajectory," *Journal of Guidance, Control, and Dynamics*, Vol. 28, No. 4, 2005, pp. 782–794. doi:10.2514/1.8433

[7] Schaub, H., Vadali, S. R., Junkins, J. L., and Alfriend, K. T., "Spacecraft Formation Flying Control using Mean Orbit Elements," *Journal of the Astronautical Sciences*, Vol. 48, No. 1, Jan.–Mar. 2000, pp. 69–87.

[8] Breger, L., and How, J. P., "Formation Flying Control for the MMS Mission Using GVE-Based MPC," *Proceedings of the IEEE Conference on Control Applications*, Inst. of Electrical and Electronics Engineers, Piscataway, NJ, Aug. 2005, pp. 565–570.

[9] Ardaens, J. S., and D'Amico, S., "Control of Formation Flying Spacecraft at a Lagrange Point," Deutsches Zentrum für Luft- und Raumfahrt TN 08-01, Wessling, Germany, Apr. 2008.

[10] McInnes, C. R., "Potential Function Methods for Autonomous Spacecraft Guidance and Control," *Advances in the Astronautical Sciences*, Vol. 90, Aug. 1996, pp. 2093–2109.

[11] McInnes, C. R., "Autonomous Ring Formation for a Planar Constellation of Satellites," *Journal of Guidance, Control, and Dynamics*, Vol. 18, No. 5, 1995, pp. 1215–1217. doi:10.2514/3.21531

[12] Gómez, G., Marcote, M., Masdemont, J. J., and Mondelo, J. M., "Zero Relative Radial Acceleration Cones and Controlled Motions Suitable for Formation Flying," *Journal of the Astronautical Sciences*, Vol. 53, No. 4, Oct.–Dec. 2005, pp. 413–431.

[13] Beard, R. W., and Hadaegh, F. Y., "Fuel Optimization for Unconstrained Rotation of Spacecraft Formation," *Journal of the Astronautical Sciences*, Vol. 43, No. 3, 1999, pp. 259–273.

[14] Vicsek, T., Czirok, A., Ben-Jacob, E., Cohen, I., and Sochet, O., "Novel Type of Phase Transition in a System of Self-Driven Particles," *Physical Review Letters*, Vol. 75, No. 6, Aug. 1995, p. 1226. doi:10.1103/PhysRevLett.75.1226

[15] Shen, J. J., "Cucker–Smale Flocking Under Hierarchical Leadership," *SIAM Journal on Applied Mathematics*, Vol. 68, No. 3, 2007, pp. 694–719. doi:10.1137/060673254

[16] Fridlund, C., "Darwin–The Infrared Space Interferometry Mission," *ESA Bulletin*, Vol. 103, Aug. 2000, pp. 20–25.

[17] Szebehely, V., *Theory of Orbits*, Vol. 1, Academic Press, New York, Mar. 1967.

[18] Gómez, G., Marcote, M., Masdemon, J. J., and Mondelo, J. M., "Natural Configurations and Control Strategies Suitable for Formation Flying," AAS/AIAA Astrodynamics Specialist Conference, Lake Tahoe, CA, American Astronautical Society Paper 05-347, 2005.